INFLUENCE OF NONIONIC SURFACTANT MOLECULAR COMPOSITION ON THE HYGROSCOPIC GROWTH OF SUPERMICRON NACL

by

ABIGAIL E. HOBBS

(Under the Direction of Amanda A. Frossard)

ABSTRACT

The effects of specific properties of surfactants on the hygroscopic growth of supermicron aerosol in the atmosphere are not well understood. Nonionic surfactants have been shown to enhance aqueous aerosol hygroscopic growth, but further investigation is needed to determine the role that chemical and physical properties of the nonionic surfactants play in facilitating water uptake. In this study, we investigate the hygroscopic growth of aqueous supermicron NaCl aerosol particles containing small mass fractions of three distinct nonionic surfactants using an Aerosol Optical Trap coupled with cavity-enhanced Raman spectroscopy. Here, we show that all nonionic surfactants in this study contributed to more particle hygroscopic growth at high surfactant concentrations, compared to particles with NaCl only. Additionally, when a small mass fraction of the water-soluble organic glucose was added to the particles with surfactant and NaCl, the hygroscopic growth decreased to that of the NaCl only particles, essentially removing any influence of the surfactants. Together, this shows that it is important to consider the total composition of the particle when modeling supermicron particle hygroscopic growth.

INDEX WORDS: hygroscopic growth, supermicron aerosol, single particle, Raman spectroscopy, Aerosol Optical Trap, nonionic surfactants

INFLUENCE OF NONIONIC SURFACTANT MOLECULAR COMPOSITION ON THE HYGROSCOPIC GROWTH OF SUPERMICRON NACL PARTICLES

by

ABIGAIL E. HOBBS

B.S., University of Georgia, 2023

A Thesis Submitted to the Graduate Faculty of The University of Georgia in Partial Fulfillment of the Requirements for the Degree

MASTER OF SCIENCE

ATHENS, GEORGIA

2025

INFLUENCE OF NONIONIC SURFACTANT MOLECULAR COMPOSITION ON THE HYGROSCOPIC GROWTH OF SUPERMICRON NACL PARTICLES

by

ABIGAIL E. HOBBS

Major Professor:	Amanda A. Frossard
Committee:	Geoffrey Smith
	Rawad Saleh

Electronic Version Approved:

Ron Walcott
Vice Provost for Graduate Education and Dean of the Graduate School
The University of Georgia
December 2025

DEDICATION

To all the people I love: thank you for being there for me during this wild ride and your unconditional support. I could not have done this without all the people I have met and cared for along the way.

TABLE OF CONTENTS

Page

LIST OF TABLES

Page

LIST OF FIGURES

Page

CHAPTER 1

INFLUENCE OF NONIONIC SURFACTANT MOLECULAR COMPOSITION ON THE HYGROSCOPIC GROWTH OF SUPERMICRON NACL PARTICLES

Abigail E. Hobbs and Amanda A. Frossard. To be submitted to *Aerosol Science and Technology*.

ABSTRACT

Understanding the mechanisms that control supermicron particle hygroscopic growth in the atmosphere is important when predicting aerosol-cloud interactions. The influence of physicochemical properties of surfactants on the hygroscopic growth of supermicron aerosol in the atmosphere is not well understood. Nonionic surfactants have been shown to enhance aqueous aerosol water uptake, but further investigation is needed to determine the role that surfactant molecular composition, structure, topological surface area, and interfacial properties play. In this study, we investigate the hygroscopic growth of aqueous supermicron NaCl aerosol particles containing small fractions three distinct nonionic surfactants using an Aerosol Optical Trap coupled with Raman spectroscopy. The dynamic surface tensions of corresponding solutions were measured with a Bubble Pressure Tensiometer. Here, we show that certain nonionic surfactants in this study contributed to more particle hygroscopic growth, compared to that NaCl only particles. This degree of enhanced hygroscopic growth was dependent on the concentration of surfactant but did not vary significantly with different surfactant molecular compositions, as did the dynamic surface tension. Additionally, when a small fraction of the water-soluble organic glucose was added to the particles with surfactant and NaCl, the hygroscopic growth decreased to that of the NaCl only particles, essentially removing any influence of the surfactants. Alone, this small fraction of glucose would not change the hygroscopic growth of NaCl particles. Together, this shows the importance to consider the total composition of the particle when modeling supermicron particle hygroscopic growth.

1. Introduction

Aerosol particles are ubiquitous in the atmosphere and can have different effects on the Earth's climate depending on their chemical composition, size, lifetime, and morphology (Lewis and Schwartz 2004; Paramonov et al. 2013; Jimenez et al. 2009). Aerosol particles can directly influence climate by scattering solar radiation and cooling the Earth's surface as well as absorbing solar radiation and warming the atmosphere (Yu et al. 2006; Haywood and Shine 1995; Haywood and Boucher 2000). Additionally, aerosol particles can indirectly affect the climate by acting as cloud condensation nuclei (CCN) or ice nuclei (IN) and contribute to the formation of water or ice clouds (Lohmann and Feichter 2005; Quinn et al. 2015; Abbatt et al. 2006; Knopf, Alpert, and Wang 2018; English et al. 2014). The overall influence of aerosol particles on Earth's radiative balance is still highly uncertain, with a large range in modeled effects, mainly attributed to aerosol-cloud interactions and requires further investigation to constrain the factors that govern CCN activation into cloud droplets and subsequent particle growth (Intergovernmental Panel on Climate 2014).

Both the indirect and direct effects of aerosol particles on the climate are dependent on the particle size and chemical composition which vary depending on source and production mechanism. While most CCN are submicron particles, supermicron particles also contribute to the scattering and absorbing of solar radiation (Kleefeld et al. 2002). Additionally, supermicron particles are generally more hygroscopic (Zhang et al. 2014). These particles can contribute to fog formation and haze at atmospheric relative humidities less than 100%, having a strong influence on visibility and fog composition at lower elevations (Mazoyer et al. 2019).

The largest source of naturally emitted aerosol particles to the atmosphere is sea spray aerosol (SSA) (Lewis and Schwartz 2004; de Leeuw et al. 2011), and it is a major source of supermicron particles in the atmosphere (Quinn et al. 2015; Lewis and Schwartz 2004). Once in the atmosphere, supermicron SSA hygroscopic growth, or the ability for a particle to uptake water from its surroundings, is largely controlled by size and chemical composition both which influence the magnitude that supermicron particles will contribute to indirect climate effects(Lewis and Schwartz 2004; de Leeuw et al. 2011; Quinn et al. 2015). The chemical composition of SSA is dependent on size and production pathway. Submicron sized particles (< 1 μm) are dominated by an organic fraction while super-micron particles (> 1 μm) are primarily comprised of inorganic sea salts such as sodium and chloride that along with a small fraction of organics(Quinn et al. 2015; Lewis and Schwartz 2004; de Leeuw et al. 2011). Previous studies of SSA have shown the organic fraction to be ~30-60% of particle mass in submicron particles and ~2-4% of particle mass in supermicron particles(O'Dowd and de Leeuw 2007; O'Dowd et al. 2004). Some studies have observed the organic fraction of SSA to contain surfactants and represent approximately 3% of the total particle mass(Frossard et al. 2019; Gérard et al. 2016). Surfactants have previously been quantified in aerosol particles collected across different ambient coastal environments(Burdette et al. 2023; Gérard et al. 2016). Specifically, a recent field study observed that for supermicron particles of marine influence and a mix of continental and marine origin, the organic fraction was comprised of approximately 62-72% surfactant-like compounds and were present in sufficiently high concentrations to lower the bulk surface tension measurements(Burdette et al. 2023). This shows that surfactants are present in atmospheric aerosol and further emphasizes the importance to elucidate their influence on supermicron particle microphysics.

Surfactants are a unique subclass of organic compounds with amphiphilic structures and interfacial properties. When surfactants are present in solution, they reduce both the free-energy and interfacial tension(Diamant, Ariel, and Andelman 2001; Xi Yuan and Rosen 1988; Eastoe and Dalton 2000). At sufficiently high concentrations, surfactants aggregate at interfaces and disrupt the hydrogen bonding of water molecules at the air-solution boundary, altering the interfacial tension(Eastoe and Dalton 2000; Xi Yuan and Rosen 1988). As surfactant concentrations increase, excess surfactant in the bulk solution that cannot partition to the saturated surface begin to self-aggregate into micelles, at the critical micelle concentration (CMC) in the bulk phase(Cui et al. 2008; Maibaum, Dinner, and Chandler 2004). As surfactant concentration increases, the surface tension will decrease until the CMC is reached. Specifically, the topological polar surface area (TPSA) of the head group, ionicity and molecular composition (i.e. functionalization of the carbon chain) all affect the partitioning behavior of surfactants in aqueous environments(Rosen 1972; Hua and Rosen 1991; Attwood 2009).

In recent studies, ionic surfactants (cationic and anionic) were found to have no influence on the hygroscopic growth of single, supermicron aerosol particles, compared to those particles containing only NaCl(Swanson and Frossard 2022). However, particles containing nonionic surfactants in addition to NaCl had an enhancement in water-uptake under the same experimental conditions(Swanson and Frossard 2022). Surfactant ionicity plays a role in aerosol particle hygroscopicity, where salting out caused by the interaction of the ionic surfactants and the dissolved ionic salts can influence micelle formation and surface tension depression by lowering

the CMC value and increasing the surfactant efficiency(El Haber et al. 2023; Attwood 2009; Rosen 2004). However, nonionic surfactants do not exhibit the same salting out effects in bulk solutions but do influence supermicron NaCl particle water uptake(El Haber et al. 2023; Rosen 2004). The lack of ionic character and minimal interactions with co-solutes observed with nonionic surfactants demonstrates a need for further investigation into the mechanism that controls water uptake of particles containing nonionic surfactants. The physical and chemical properties of nonionic surfactants, such as their molecular weight, structure, and TPSA may play a role in their influence on the hygroscopic growth of supermicron aerosol particles.

Surfactants have varying effects on aqueous solutions depending on the size regime of the system (i.e. microscopic versus macroscopic). The large surface-area-to-volume ratio of aerosol particles requires that the bulk depletion of surfactants from the particle bulk to the air-particle boundary should be incorporated when evaluating the hygroscopic growth behavior of supermicron particles(Bain et al. 2024; Bain et al. 2023; Bzdek et al. 2020; Jacobs, Johnston, and Mahmud 2024). In microscopic aerosol systems, surfactant molecules will partition from the bulk particle phase and aggregate at the particle surface leaving the bulk phase depleted of surfactants and overall increasing the activity of water giving a surface tension that is greater than the parent solution from which it was atomized(Bain et al. 2023; Jacobs, Johnston, and Mahmud 2024). This change in the bulk solute composition of particles can have opposing effects when also considering the influence of interfacial tension. Advancements in single aerosol surface tension and hygroscopic growth instrumentation have provided a pathway to compare experimental results to predictions using Köhler theory that incorporates more complex parameters for the physical

properties of aerosol (e.g. bulk-depletion, size, etc.)(Köhler 1936; Werner, Hammond, and Bain 2025; Gen et al. 2023).

Single particle measurements are of importance to better constrain the microphysical properties that affect aerosol water uptake(Swanson and Frossard 2022; Frossard et al. 2018; Bain 2024). To evaluate simpler systems and isolate surfactant effects, laboratory experiments have been done to evaluate the changes in hygroscopic growth when surfactants are added to aqueous NaCl supermicron particles (Bain et al. 2024; Swanson and Frossard 2022; Frossard et al. 2018) using a proven method that utilizes an aerosol optical trap(Mitchem et al. 2006; Hopkins et al. 2004; Summers, Reid, and McGloin 2006; Mitchem and Reid 2008; Knox et al. 2007). This study found that ionicity of the surfactant plays a role in the subsequent hygroscopic growth of surfactant-containing particles with a 3% increase in water uptake only by nonionic surfactant containing NaCl particles(Swanson and Frossard 2022). It has also been observed that at sufficiently high surfactant concentrations, trapped particles will rapidly evaporate in sub-saturated humidity conditions(Swanson and Frossard 2022; Frossard et al. 2018). Recent single particle experiments have observed that the addition of ionic surfactants to supermicron particles at atmospherically relevant concentrations (~0.1-12 mM) can alter the interfacial properties and lead to a surface tension depression that has a strong correlation with surfactant concentration (Jacobs, Johnston, and Mahmud 2024). Recent studies are revealing a need to further constrain the influence of surfactants on single supermicron particle hygroscopic growth and microphysics to better quantify and predict their influence on climate and visibility.

In this study, we evaluate the impact of nonionic surfactant molecular composition and weight on supermicron model SSA hygroscopic growth using an aerosol optical trap coupled with cavity-enhanced Raman spectroscopy. Additionally, we investigate the influence of varying solute composition and concentration on particle hygroscopic growth and surface tension dynamics. Nonionic surfactant strength and partitioning timescales was analyzed using dynamic surface tension measurements for each experimental condition. Coupling these two measurements allows for connections between bulk surface activity (i.e. dynamic surface tension) and hygroscopic growth of model SSA across multiple surfactant concentrations and organic compositions to be investigated.

2. Experimental Methods

2.1 Model SSA composition and concentration

Aqueous aerosols were generated from nine different solutions covering a range of composition and concentration to model atmospherically relevant SSA particles with size-dependent organic and inorganic fractions (Quinn et al. 2015; Keene et al. 2007; O'Dowd and de Leeuw 2007). Supermicron aerosol of marine origin are primarily composed of inorganic sea salts but have been observed to contain an organic fraction (~2-4% by mass) (O'Dowd and de Leeuw 2007; Bertram et al. 2018; Keene et al. 2007). To address the influence of nonionic surfactants on aerosol hygroscopic growth, two model systems were evaluated i) water soluble nonionic surfactants were added to solution with sodium chloride (NaCl) at 0.5-1.5% mass fractions with the remaining solute fraction being NaCl (simple) and ii) water soluble nonionic surfactant and organic compounds (glucose) were added in a 1:1 mass ratio to solution with NaCl which constitutes the remaining solute mass fraction (complex). NaCl in our study broadly represents the inorganic salts

found in marine aerosol due to its abundance in both SSA and seawater (Lewis and Schwartz 2004; Keene et al. 2007; Miyazaki et al. 2018; Vaccaro et al. 1968).

In the simple, NaCl-surfactant solution(s), nonionic surfactants are added at two mass fractions to address differences in aerosol surface and bulk composition across varying concentrations. In all solutions, the NaCl mass fraction is kept constant at ~97.5% to minimize variations in water up-take due to the highly hygroscopic nature of NaCl. For the complex, NaCl-surfactant-glucose solutions, the mass of surfactant was chosen based on the observed enhancement in water up-take measured for aerosol generated from the NaCl-surfactant particle experiments at the 1.3-1.5% mass fraction (~0.015 g). Glucose was then added to solution in a 1:1 mass ratio (~0.015 g) for each of the three nonionic surfactants in our study. Each of the aqueous solutions were individually transferred to the atomizer only prior to the start of the experiment. It is assumed that as the solution is atomized the ratio of solutes is conserved (Bzdek et al. 2020).

The nonionic surfactants used in this study were selected to elucidate molecular features (i.e. molecular weight, functional group composition, etc.) that facilitate an enhancement of up-take of water by supermicron model SSA. Tergitol NP-40, Brij 35, and Brij L4 were the nonionic surfactants measured due to their wide variation in molecular composition and weight. Notable physical properties, structures, and concentrations of surfactants for each solution are shown in Table 1.

Table 1. Physical and chemical properties of the nonionic surfactant and glucose standards used in this study, including molecular weight (MW), critical micelle concentration (CMC), water solubility, and topological polar surface area (TPSA).

Compound	Molecular Structure	MW (g mol^{-1})	CMC (mM)	Water Solubility	TPSA ($Å^2$)[h]
Brij L4	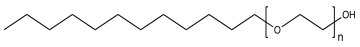	362 average[a]	0.039[d]	soluble	57.2
Brij 35	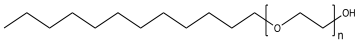	1199 average[b]	0.09[e]	40 mg/mL[g]	233
Tergitol NP-40	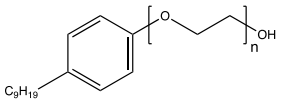	1980 average[c]	0.23[f]	soluble	196
Glucose	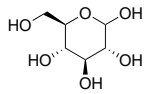	180.15	N/A	soluble	110

[a]Average n of 4.
[b]Average n of 23.
[c]Average n ranging from 39-40.
[d](Warmbier et al. 2024)
[e](Koneva et al. 2018)
[f]Sigma-aldrich, 232 mg/L
[g]Bioworld Molecular Tools and Laboratory Essentials
[h]Topological polar surface area (TPSA) values listed in the table were provided by PubChem and calculated using Cactvs 3.4.8.18

2.2 Single aerosol hygroscopic growth measurements

The hygroscopic growth of aqueous particles composed of NaCl only were used as a proxy for the inorganic fraction of SSA. The inorganic composition of seawater consists largely of sodium and chloride ions indicated by their salinity mass ratios 10.78 and 19.35 g/kg_{sw}, respectively (Lewis et al. 2004). Model seawater solutions were atomized (TSI, Single Jet 3092) into a stainless-steel chamber of regulated relative humidity. Relative humidity was controlled by adjusting the dry and/or wet clean air flows (Bretchel Manufacturing Prehumidifier) into the chamber that were introduced at a flow rate of ~0.2-0.3 LPM or less to minimize disturbance of the trapped particle. Throughout each experiment the relative humidity was monitored with a sensor (± 3% uncertainty, Elitech GSP-6G) placed through a port on the trapping chamber and was situated approximately 2

cm away from the beam waist. The duration of droplet measurements was 10 minutes, and the RH was controlled to ±0.8% of the target RH for the duration.

The hygroscopic growth for supermicron NaCl particles was measured using a custom-built aerosol optical trap combined with cavity-enhanced Raman spectroscopy(Haddrell et al. 2017; David et al. 2020; Swanson and Frossard 2022; Frossard et al. 2018). Briefly, aerosols are introduced into the stainless-steel chamber under nearly saturated relative humidity conditions (~90% RH). As aqueous aerosols enter the chamber and conditions, a single aerosol will become optically trapped as it crosses the beam waist and simultaneously excited by a 514 nm CW laser (Coherent, Genesis MX514-STM). The laser light propagates through the optical path and is then focused through a 1.2 numerical aperture microscope objective (Olympus, 60x, water immersion, working distance 0.28 mm) to create the working optical trap in the stainless-steel chamber. Raman backscattered light is focused into a 0.5 m spectrometer (SpectraPro HRS-500S, diffraction grating 1200 grates/mm) coupled to a 0.03 mm resolution CCD detector (Princeton Instruments, PIXIS 100F). In real time, images of the aqueous particles are captured using brightfield microscopy with a 455 nm LED for illumination paired with a CMOS camera (Imaging Source, Monochrome).

Determination of single aqueous aerosol size and refractive index is accomplished using cavity-enhanced Raman spectroscopy (CERS). In this study, single aerosols with radii of 2-4 μm were stable in the optical trap and reproducible CERS measurements were observed. Aerosol size and refractive index was extracted by matching peaks in the experimental Raman spectra to those predicted by Mie theory of particles in the same size range(Frossard et al. 2018; Wills, Knox, and Reid 2009; Hopkins et al. 2004). The size, wavelength, and structure of the Raman resonant bands,

whispering gallery modes (WGMs), are indicative of the trapped particle refractive index and size. Throughout each experiment, the whispering gallery modes were monitored in real-time to denote any potential changes to particle size that did not correspond to a change in chamber relative humidity.

Aerosol particles were introduced and optically trapped under near saturated RH conditions (~88-92% RH). In this experiment, CERS measurements were taken at discrete RH steps of 80 and 70% RH to evaluate changes in water up-take by aerosols under atmospherically relevant sub-saturated conditions(Swanson and Frossard 2022; Frossard et al. 2018). The chamber was lowered from ~90% RH down to 80 ± 1% RH to begin the humidity cycling process. For the 70% RH step, the chamber conditions were lowered by exactly 10% (e.g. if the first step was 80.4% RH the second step was 70.4% RH). Following successful trapping and RH adjustments, each particle was allowed to come to equilibrium (~5-7 minutes) before the measurement began to minimize undesired changes in particle size. After the 80% RH measurements were taken, the same process was repeated at the 70% RH step. Raman spectra were collected continuously for the duration covering the 600 to 640 nm wavelength range (centered at 621 nm). The particle was determined to be at equilibrium within the chamber once the real-time whispering gallery modes were stable in the Raman spectrum. For surfactant containing particles, the equilibration time at each RH step also ensured that surfactant aggregation at the particle surface occurred. Aqueous particles containing 611 mM NaCl were used as a reference value and calibration setpoint throughout the project. NaCl has been extensively studied to compare our hygroscopic growth measurements to, allowing for an accurate comparison and validation method(Tang, Tridico, and Fung 1997; Lewis and Schwartz 2004; Swanson and Frossard 2022; Frossard et al. 2018).

The hygroscopic growth of single supermicron aerosol was quantified by calculating the hygroscopic growth factor ($r_{70/}r_{80}$) which we define as the ratio of the radius at 70% relative humidity to the radius at 80% relative humidity. For each single particle, a 10-minute CERS measurement is performed at each discrete RH step, and the radius is reported as the average radius ± standard deviation for the duration of the Raman measurement. Calculated hygroscopic growth factors are shown in Table 2. For each model seawater solution, 2-11 particles were trapped and their respective $r_{70/80}$ values are reported in Table 2.

2.3 Dynamic surface tension of model seawater

Bulk dynamic surface tension measurements were performed on the macroscopic model seawater solutions to probe the interfacial properties and timescales at which nonionic surfactants aggregate to interfaces in multi-component solutions. To evaluate surfactant interfacial properties as a function of time, bubble pressure tensiometry (Krüss Scientific, BPT Mobile) was used. Briefly, a needle tip is lowered just below the solution surface where gas bubbles are generated and held for discrete time intervals. The pressure required to sustain a stable gas bubble below the solution surface, for specific and defined bubble ages, is related to the interfacial properties of the solution itself (Eastoe and Dalton 2000; Holcomb and Zollweg 1992). The surface tension depression is used to describe surfactant strength and is define as the change in surface tension with the addition of nonionic surfactants when compared to the surface tension of pure water.

To assess how surfactant molecular composition influences surface activity, all two and three component model seawater solutions have dynamic surface tension curves and corresponding $r_{70/80}$

values (Table 2). The dynamic surface tension was measured as a function of time (bubble age) ranging from 10 to 30,000 ms. As a baseline and calibration parameter, dynamic surface tension curves for ultra-pure water (18 MΩ conductivity) were measured prior to each sample solution. All model seawater solutions were made with 18 MQ ultra-pure water, so the surface tension depression for each solution with the addition of nonionic surfactants and water-soluble organic compounds can be determined. Prior to the measurement, all solutions were allowed 15-20 minutes to reach room temperature (~22-24 °C) to minimize the influence of temperature on surface tension. The surface tension of each solution was measured in triplicate, and the average of the measurements with their corresponding standard deviation is reported in Figure 2.

In our study, dynamic surface tension is used to probe the timescale at which nonionic surfactant molecules partition at interfaces. Here, the bubble age (ms) is analogous to surfactant concentration and is shown in the surface tension curves (Figure 2). As the gas bubble is held below the solution surface, the calculated surface tension is greatly influence by the bubble age. As bubble age increases, a greater number of surfactant molecules are able to aggregate at the bubble-solution boundary resulting in a greater surface tension depression when surface-active compounds are present. This bulk surface tension method provides insight into time-dependent surfactant interfacial properties, as well as the influence of water-soluble organic compounds on surface tension in the presence of surfactants. This study utilizes coupled dynamic surface tension measurements with $r_{70/80}$ calculations to better constrain how both aerosol chemical composition and surfactant molecular composition influence hygroscopic growth of coarse mode model SSA systems.

3. Results and Discussion

3.1 ***Hygroscopic growth of supermicron aqueous NaCl particles***

The mean growth factor ratio (r_{70}/r_{80}) measured in this study for aqueous aerosol particles containing NaCl only is 0.923 ± 0.015 (n=11). This mean value is similar to previous measurements of r_{70}/r_{80} using a similar aerosol optical trap instrument (mean of 0.902 ± 0.007 from Swanson et al., 2022; and median of 0.88 ± 0.06 from Frossard et al. 2018) and falls within the corresponding standard deviation ranges. Additionally, previous studies of supermicron model sea salt particles show r_{70}/r_{80} of 0.91 (Tang, Tridico, and Fung 1997) which is also within our measured standard deviation. This measured r_{70}/r_{80} is also similar to that calculated by Kohler Theory (0.90) and the extended AIM model (0.91) for particles containing only NaCl in this size range(Köhler 1936; Clegg, Seinfeld, and Brimblecombe 2001). These measurements were collected for NaCl only particles at the start and end of each experimental condition, throughout the study. The small standard deviation (± 0.015) indicates good reproducibility between particle measurements and supports minimal variability introduced from small changes in instrumental conditions (i.e., temperature) throughout the experiments, as well as error in the measurements of the relative humidity. The NaCl only particles measured in this study ranged in diameter from at 70% RH, and the r_{70}/r_{80} showed no trend with particle size.

3.2 Nonionic surfactants influence hygroscopic growth of single NaCl particles

In this experiment, we measured the influence of three different nonionic surfactants, each at two or three different concentrations (listed in **Table 2**) on the hygroscopic growth of aqueous NaCl particles. The measured particle radii at 70% (r70) and 80% (r80) RH were used to calculate the r_{70}/r_{80} and compared across the experimental conditions and to our baseline conditions using NaCl.

The mean r_{70}/r_{80} for particles containing NaCl and one nonionic surfactant (NaCl-surfactant particles) at different solute mass fractions are reported in **Table 2** and shown in **Figure 1.** In these experiments, the r_{70}/r_{80} is dependent on nonionic surfactant concentrations, as well as surfactant composition.

Table 2. Concentrations of each nonionic surfactant, organic mass fraction, number of particles trapped, and mean measured (r_{70}/r_{80}) ± standard deviation for the three experimental conditions

Experiment	Nonionic Surfactant Conc. (mM)	Organic Mass Fraction of PM (%)[a]	Surfactant Conc. Rel. to CMC	Number of particles	Mean r_{70}/r_{80} ± standard deviation	t-Test at 99% confidence[b]
NaCl only						
NaCl only	N/A	N/A	N/A	11	0.923 ± 0.015	N/A
NaCl + surfactant						
Tergitol NP-40	8.99	0.8	~27x	7	0.916 ± 0.009	ns
	16.78	1.5	~73x	2	0.886 ± 0.019	*
Brij L4	52.00	0.8	~130x	7	0.902 ± 0.019	ns
	81.27	1.3	~2000x	4	0.887 ± 0.006	*
Brij 35	10.59	0.5	~118x	6	0.890 ± 0.024	*
	26.32	1.5	~292x	7	0.931 ± 0.017	ns
	44.43	2.5	~494x	3	0.898 ± 0.020	ns
NaCl + surfactant + glucose						
Tergitol NP-40 + glucose	16.57	3.0	~72x	6	0.914 ± 0.018	ns; *
Brij L4 + glucose	92.09	3.0	~2300x	7	0.921 ± 0.016	ns; *
Brij 35 + glucose	27.85	3.0	~309x	2	0.908 ± 0.015	ns; ns

[a]For NaCl-surfactant-glucose particles, the mass fraction listed is the total organic mass fraction including a 1:1 mixture of surfactant and glucose

[b]Statistical differences of the sample mean r_{70}/r_{80} compared to the NaCl only particles (* indicates a significant difference with 99% confidence, and ns indicates no significant difference); sample means for the experiments with glucose are also compared to the corresponding sample means of the NaCl and surfactant particles for the same surfactant mass fraction (indicated with a second * or ns).

3.2.1 Tergitol NP-40 and Brij L4

For NaCl-surfactant particles, when Tergitol NP-40 is the surfactant fraction, we observe a concentration dependent r_{70}/r_{80}. At 0.5% surfactant mass fraction (i.e., lower concentration condition), for NaCl-Tergitol NP-40 particles the mean r_{70}/r_{80} of 0.916 ± 0.009 is not significantly different from that of NaCl only particles, with a mean r_{70}/r_{80} of 0.923 ± 0.015 (**Table 2**), indicating that very small fractions of the surfactant Tergitol NP-40 do not change the particle hygroscopic growth. However, when the surfactant mass concentration was increased to 1.5% (i.e., higher concentration condition) for the NaCl-Tergitol NP-40 particles, the mean r_{70}/r_{80} was 0.886 ± 0.010,

which is statistically significantly lower than that of the NaCl only particles (**Table 2**). This decrease in mean r_{70}/r_{80} compared to that of NaCl only particles indicates an increase in hygroscopic growth for particles containing higher mass fractions of surfactants.

We observe a similar concentration dependent hygroscopic growth trend for NaCl-surfactant particles containing Brij L4 as the nonionic surfactant fraction. The similar hygroscopic growth behavior is unexpected as Brij L4 represents the simplest molecular complexity and smallest molecular weight, while Tergitol NP-40 is the largest and most complex nonionic surfactant in our study. At lower surfactant mass fractions (0.5% Brij L4; lower concentration condition), the mean r_{70}/r_{80} of 0.902 ± 0.019 does not differ significantly from that of the NaCl only particles (**Table 2**). However, similarly to Tergitol NP-40, when the surfactant mass fraction of Brij L4 is increased to 1.5% (i.e., higher concentration condition), the r_{70}/r_{80} for NaCl-Brij L4 particles (mean r_{70}/r_{80} of 0.887 ± 0.006) was statistically significantly lower than that of NaCl only particles (**Table 2**). This shows an enhancement in water uptake and higher hygroscopic growth by NaCl-Brij L4 particles at higher surfactant concentrations.

The concentration dependent hygroscopic growth of the NaCl-surfactant particles containing Tergitol NP-40 or Brij L4 suggests that larger mass fractions of surfactants (observed at 1.5%) facilitate an enhanced water uptake compared to the NaCl only particles. The concentration dependent hygroscopic growth has been previously observed for NaCl-surfactant particles containing the nonionic surfactant Tergitol NP-40 (Swanson and Frossard 2022). In that study, no statistically significant increase in hygroscopic growth was observed until the Tergitol NP-40 mass fraction was greater than ~0.2%, which was at a concentration in the particle larger than three

times the CMC(Swanson and Frossard 2022). Additionally, Frossard et al. (2018) also observed a concentration dependent hygroscopic growth for NaCl particles containing nonionic surfactant Triton X-100, with larger deviations in r_{70}/r_{80} as the fraction of Triton X-100 was increased.

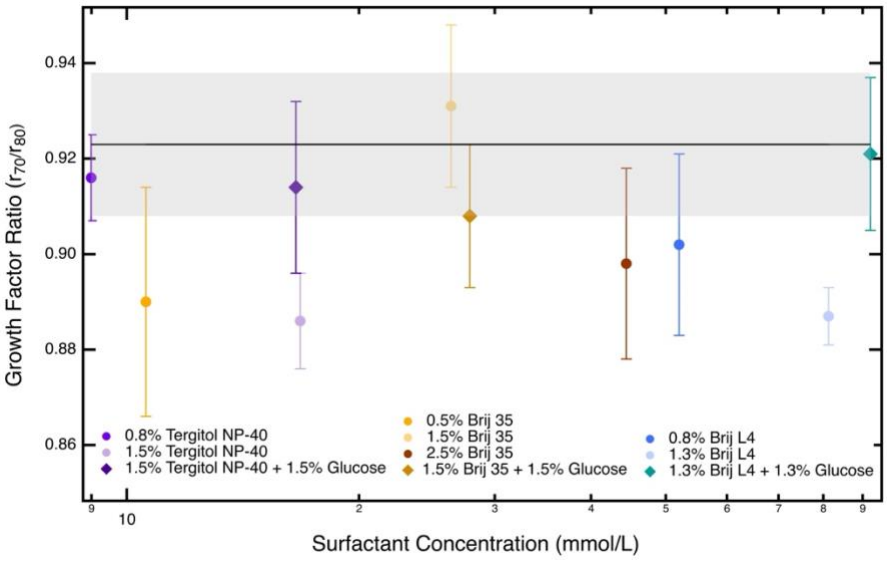

Figure 1. Comparison of mean hygroscopic growth (r_{70}/r_{80}) of aqueous particles, including NaCl-surfactant particles with different surfactant concentrations (circles) and NaCl-surfactant-glucose particles (diamonds). Mean r_{70}/r_{80}values are shown for each particle type, and the error bars correspond to the standard deviation. The solid black line is the experimentally measured mean $r_{70}/r_{80}$for 611 mM NaCl particles, and the shaded region represents the standard deviation (± 0.015).

Taken together, the statistically different mean r_{70}/r_{80} of NaCl-surfactant particles compared to NaCl only particles at higher surfactant mass fractions for Tergitol NP-40 and Brij L4 may be due to the effective concentrations of surfactants in the bulk of the particles. At lower surfactant mass fractions (0.5%), the NaCl-surfactant particles containing Tergitol NP-40 and Brij L4, bulk depletion may have been be playing a role in mediating water uptake, making the hygroscopic growth and mean r_{70}/r_{80} similar to that of pure water. Surfactants are surface-active and will aggregate at air-liquid interfaces, such as the particle-air interface. The aggregation of surfactants on the surface of the particles effectively lowers the surfactant concentration in the bulk phase, compared to the total concentration of surfactants in the particle. As surfactants partition to this interface, the activity of water increases which in turn changes the physical and chemical properties

of the aerosol (Bain et al. 2024; Bain et al. 2023; Clegg, Seinfeld, and Brimblecombe 2001; Zuend et al. 2008). In this study, the effective concentration of surfactants in the bulk of the particle is not large enough to alter the r_{70}/r_{80} and hygroscopic growth of the NaCl-surfactant particle until the surfactant fraction of Tergitol NP-40 or Brij L4 is 1.5% or greater.

Under both lower and higher concentration conditions, for NaCl-surfactant particles containing nonionic surfactants Tergitol NP-40 or Brij L4, the particle surface is predicted to be saturated with surfactant molecules, throughout the experimental RHs measured here (Figure S1). Surfactants form monolayer coverage at the particle-air boundary leading to a core-shell structured phase separation. Using the concentrations and the individual physical properties of Tergitol NP-40 and Brij L4, including molecular weight, density, and TPSA, Figure S1 shows that the predicted NaCl-surfactant particle surface area coverage is greater than 100%. As expected, Figure S1 shows the surface area coverage to be much higher than 100% for particles containing larger Tergitol NP-40 or Brij L4 mass fractions of 1.5%, indicating that at that concentration, there is a significant concentration of surfactant in the bulk of the particle, which may contribute to the differences in mean r_{70}/r_{80} for the low and high concentration conditions. This suggests that the larger excess surfactant in the bulk particle phase controls the hygroscopic growth of the NaCl-surfactant particles.

At surface area coverage values greater than 100%, excess surfactant is in the bulk phase, which can self-aggregate into micelles, depending on if the effective surfactant concentration in the bulk is greater than the CMC of the solution (Rosen 1972, 2004; Maibaum, Dinner, and Chandler 2004; Bain et al. 2024). Formation of micelles changes the bulk composition of the aerosol and

effectively lowers the activity of water. For both the lower and higher concentration conditions for NaCl-surfactant particles containing Tergitol NP-40 or Brij L4, the total concentrations of surfactants in the particle are much larger than the corresponding CMCs (Table 2), and the predicted surface area coverage for each is much greater than 100% (Figure S1). This suggests that the concentrations of surfactants in the bulk phase may be high enough to form micelles, especially at the higher concentration conditions. While salts can lower the CMC of ionic surfactants, they do not affect the CMC of nonionic surfactants, thus indicating that the literature CMC values for these surfactants should be unchanged in these particles. Previous studies have shown that micelle formation in the bulk phase of the particle may contribute to water up-take by the particle(Swanson and Frossard 2022; Frossard et al. 2018; Werner, Hammond, and Bain 2025), consistent with our measurements.

To evaluate the influence of surfactant strength and molecular composition on $r_{70/r80}$ and particle hygroscopic growth, the bulk dynamic surface tension for each initial solution was measured (**Figure 2**). This measurement provides insight into the timescale at which surfactants partition as a function of bubble age (ms). Overall, we observe clear differences in surfactant strength in the different solutions, based on the magnitude of the surface tension depression of each solution containing surfactants compared to the surface tension of ultra-pure water. Additionally, as the surfactant mass fraction increases, the magnitude of the surface tension depression at equilibrium bubble ages (~30 s) also increases (**Figure 2**).

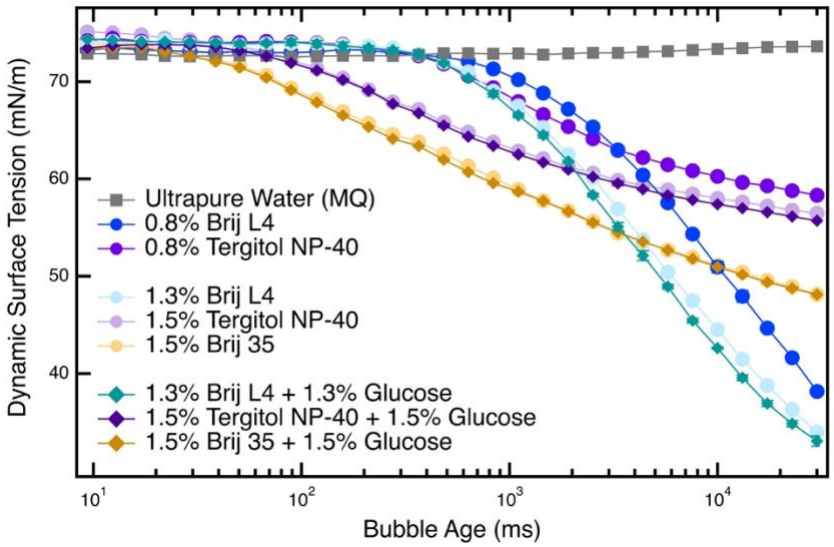

Figure 2. Mean bulk dynamic surface tension as a function of bubble age for each experiment listed in Table 2, including NaCl-surfactant (circles) and NaCl-surfactant-glucose (diamonds) solutions. The grey squares show the measured dynamic surface tension of ultra-pure water. The error bars at each data point represent the standard deviation, which is smaller than the markers for most measurements.

For NaCl-Brij L4 and NaCl-Tergitol NP-40 solutions, at equilibrium bubble age (~30 s), there is a clear increase in surface tension depression at the higher concentration conditions (1.5% surfactant mass fraction). This is consistent with the change in the hygroscopic growth for the higher surfactant mass fraction particles, compared to those with less surfactant concentration.

3.2.2 Brij 35

NaCl-surfactant particles containing Brij 35 showed different hygroscopic growth behavior with changes in concentration compared to that of NaCl-surfactant particles containing Brij L4 or Tergitol NP-40. When Brij 35 was 0.5% of the particle mass (i.e., lower concentration condition) the mean r_{70}/r_{80} was 0.890 ± 0.024, which is statistically significantly lower than that of NaCl only particles (**Table 2**), showing an increase in the hygroscopic growth. However, as the surfactant mass fraction was increased, the particle hygroscopic growth showed no significant difference compared to that of NaCl only particles. At the higher concentration condition (1.5% mass fraction), the mean r_{70}/r_{80} was 0.931 ± 0.017 and not statistically different from that of NaCl only

(**Table 2**). To further investigate the effect of higher concentrations of nonionic surfactants on hygroscopic growth, experiments at a third concentration condition (2.5% surfactant mass fraction) were done for NaCl-Brij 35 particles. At this highest concentration, the mean r_{70}/r_{80} of the NaCl-Brij particles was 0.898 ± 0.020 (Table 2). While this is an apparent decrease in r_{70}/r_{80} and thus increase in hygroscopicity, there were only 3 NaCl-Brij 35 particles measured at this condition, thus making the mean r_{70}/r_{80} not significantly different from that of NaCl only particles (Table 2).

The different behavior of NaCl-Brij 35 particles compared to NaCl-Brij L4 particles is unexpected but may be attributed to the differences in their molecular composition. Brij 35 and Brij L4 are structurally similar but differ in the number of repeating ethoxy constituents (average of 24 and 4, respectively; Table 1). This difference makes the chain length of the Brij 35 head group and thus its TPSA much larger than those of Brij L4 (Table 1). Additionally, the CMC value of Brij 35 is more than twice that of Brij L4 (Table 1). Taken together, the size of the head group, the overall molecular weight, and the TPSA may contribute to the difference in hygroscopic behavior of Brij 35 compared to Brij L4. If there is more potential surfactant surface area coverage at the same concentration for NaCl-Brij 35 particles compared to NaCl-Brij L4 particles, then there would be more excess Brij 35 in the particle bulk and thus more influence on the hygroscopic growth of the NaCl-surfactant particle at low concentrations.

Additionally, while Tergitol NP-40 has the largest number of repeating ethoxy groups (average n of 39-40 compared to average n of 23 for Brij 35; Table 1), the CMC of Tergitol NP-40 is more than twice that of Brij 35 (Table 1). This suggests that while the packing efficiency and surfactant surface area coverage for NaCl-surfactant particles containing these two surfactants may be

similar, the factor contributing more to the particle hygroscopic growth is the micelle formation in the bulk of the particle. For NaCl-Tergitol NP-40 particles, much higher concentrations of surfactants are necessary to have high enough concentrations in the bulk to form micelles, compared to the NaCl-Brij 35 particles which may form micelles in the bulk of the particle at much lower concentrations. Difference in CMC while surfactant packing and surface area coverage are similar may explain the difference in the influence of Brij 35 on the particle hygroscopic growth. At lower Brij 35 concentrations, there is enough concentration in the bulk of the particle to change the hygroscopic growth of the particles (Table 2). However, when the concentration is increased (1.5% and 2.5%), it may surpass that of the CMC in the bulk and form micelles. Those micelles remove unbound surfactants from the solution and in turn effectively lower the surfactant concentration, thus making the bulk of the particle more dilute and removing any effect of the surfactant on the hygroscopic growth of the NaCl-Brij 35 particles (Table 2).

Dynamic surface tension of Brij 35 solutions were also measured to investigate the influence of Brij 35 on the surface tension depression and time scales for equilibrium (Figure 2). At the higher concentration, the shape of the surface tension curve for Brij 35 in aqueous NaCl is similar to that of Tergitol NP-40 but significantly different from that of Brij L4. These trends in dynamic surface tension are likely due to the similarities and differences between Brij 35 and Brij L4 and Tergitol NP 40 discussed earlier. While Brij 35 is structurally similar to Brij L4, it has a much larger molecular weight and longer head group chain length and thus larger TPSA. Brij 35 is therefore more similar to Tergitol NP-40 in TPSA and molecular weight. This suggests that molecular weight and TPSA are controlling the shape of the dynamic surface tension curves. Larger, more complex surfactants have stronger repulsive forces in the aqueous phase due to the increase in

topological polar surface area of the hydrophobic alkyl tail region(Rosen 1972, 2004; Malila and Prisle 2018; Maibaum, Dinner, and Chandler 2004). This results in a faster partitioning rate for larger, more complex surfactants to the bubble-solution interface generating a greater surface tension depression compared to surfactants of less complexity at the bubble age (Figure 2). Tergitol NP-40 and Brij 35, with average molecular weights of ~1960 and ~1200 g/mol, respectively (Table 1), begin to partition to the bubble surface at ~100 ms bubble age at the 1.5% surfactant mass fraction (Figure 2). This is much faster than that of Brij L4 which has the lowest molecular weight and does not begin to aggregate at the bubble-solution interface and alter surface tension until bubble ages greater than 1000 ms.

Compositional complexity of the hydrocarbon chain region can also influence the packing efficiency of surfactant molecules at interfaces(Rosen 1972, 2004; Malila and Prisle 2018; Maibaum, Dinner, and Chandler 2004). Evaluating the differences in the measured dynamic surface tension depression for Brij 35 and Tergitol NP-40 containing solutions, packing efficiency appears to influence surface tension for all concentrations with Brij 35 having greater surface tension depression (ST_{dep} = 25.7 mN/m) than Tergitol NP-40 (ST_{dep} = 18.6 mN/m) at the same bubble age of XX ms (Figure 2). The structural composition of Brij 35 is simpler and less rigid in bond orientation compared to Tergitol NP-40 (Table 1), allowing a greater number of surfactant molecules to aggregate across a surface of the same dimensions.

3.3 Water-soluble organic alters hygroscopic growth of particles containing NaCl and nonionic surfactant

To more accurately reflect supermicron atmospheric marine aerosol particles, a water-soluble organic was added to the NaCl-surfactant particles, and the r_{70}/r_{80} were measured for the high surfactant concentration conditions. Overall, the mass fractions of organics, including both the surfactant and glucose, remained less than 5% of the total particle mass (Table 2). Water soluble organic species are commonly found in marine aerosol, and glucose is a common proxy. It has a low affinity to partition at interfaces, which allows us to isolate the influence of the aerosol bulk phase on single particle hygroscopic growth behavior(Bertram et al. 2018; Werner, Hammond, and Bain 2025).

The addition of glucose to the NaCl-surfactant particles at the high concentration conditions significantly changed the r_{70}/r_{80} of the NaCl-Brij L4 (mean of 0.921 ± 0.016) and NaCl-Tergitol NP-40 (mean of 0.914 ± 0.018) particles, compared to those without glucose (Figure 1; Table 2). The NaCl-surfactant-glucose particles all have mean r_{70}/r_{80} that are not statistically different from the NaCl only particles. This indicates that glucose acts to offset the effect of the surfactants in the NaCl-surfactant particles, making their hygroscopic growth indistinguishable from that of NaCl only particles. The addition of glucose affects the particle physicochemical properties and in turn, particles are less hygroscopic than their NaCl-surfactant counterparts.

At dilute glucose concentrations and in the presence of strong surfactants, as used in this study, glucose is not surface-active and does not out compete the surfactants to partition to the surface but is assumed to reside in the particle bulk(Werner, Hammond, and Bain 2025). The surfactant

mass fraction was constant across both NaCl-surfactant and NaCl-surfactant-glucose particles. The addition of glucose in such low concentrations does not change the effective concentration of surfactant or NaCl in the bulk of the particle. This suggests that the change in the NaCl-surfactant particle hygroscopic growth, with the addition of glucose, is being controlled by the composition of the particle bulk, rather than composition at the particle surface. Two possible explanations are that i) glucose is altering micelle formation and/or changing the effective surfactant concentration or shape of the micelles in the bulk phase; and/or ii) glucose is engaging in hydrogen bonding with water in the particle bulk increasing the activity of water (Rosen 2004).

For NaCl-glucose particles, the Extended Aerosol Inorganics Model (E-AIM) was used to calculate growth factors at 80% RH to demonstrate that glucose at this low of mass fraction will not affect the hygroscopic growth of aqueous NaCl particles (Clegg, Seinfeld, and Brimblecombe 2001). At the mass fraction used in this study (1.5%), glucose had no influence on the hygroscopic growth of supermicron NaCl particles. The concentration of glucose must be ~7x greater than our experimental concentrations to begin dampening hygroscopic growth in supermicron aqueous NaCl particles(Clegg, Seinfeld, and Brimblecombe 2001). Therefore, the glucose alone is not changing the mean r_{70}/r_{80} of the NaCl-surfactant particles, and it must be due to interactions between the glucose and surfactants (Figure S2). The observed increase in r_{70}/r_{80} for the NaCl-surfactant-glucose particles may be due to a change in the CMCs of the surfactants and thus the effective concentrations of dissolved surfactants in the particle bulk phase. If the glucose decreases the CMCs, the surfactants will form micelles at lower concentrations, which will decrease the concentration of dissolved surfactants in the bulk of the particle, making the surfactant fraction more dilute and making the hygroscopic growth more similar to that of pure water (Rosen 2004).

Similarly, the glucose may contribute to the "salting out" of the surfactant, partitioning the surfactant to the particle surface and decreasing the surfactant concentration in the bulk, making it more dilute.

To assess the influence of water-soluble organic compounds on interfacial tension, the dynamic surface tension curves for NaCl-surfactant-glucose solutions were measured for each surfactant mixture (Figure 2). For our macroscopic surface tension measurements, we observe no change in surface tension with the addition of glucose to the NaCl-surfactant solutions (Figure 2). All of the surface tension curves with the addition of glucose are indistinguishable from the corresponding curves of the solutions without glucose. This demonstrates that in macroscopic systems, glucose has no influence on interfacial tension and is likely due to the minimal interference or interaction of glucose with excess surfactant and micelle formation. This difference compared to the observed effects for the NaCl-surfactant particles suggests that an interaction between glucose and surfactant is driving the change in particle hygroscopic growth.

4. Conclusions

The measurements and calculations in this study show the importance of understanding the composition of atmospheric aerosol, and more specifically supermicron aerosol of marine origin, in order to calculate and predict particle hygroscopic growth. While NaCl particles are inherently hygroscopic, this study demonstrates that the specific composition and properties of the organic fraction can increase the hygroscopic growth of supermicron NaCl particles. Even at very small mass fractions, nonionic surfactants added to NaCl particles increased particle hygroscopicity, but the addition of glucose to the NaCl-surfactant particles reduced this effect.

Here, we evaluated the influence of three nonionic surfactants with different molecular compositions on the hygroscopic growth of single, supermicron aqueous NaCl particles. We then evaluated the influence of the addition of a water-soluble organic (glucose) to the particles containing the different surfactants and NaCl. These particles, with large fractions of NaCl (>95%) and small fractions of surfactant or surfactant mixed with glucose (<5%), were used to model supermicron SSA.

For the simple, model SSA, consisting of NaCl plus a small organic fraction of only surfactant, there was more hygroscopic growth for these particles compared to particles containing NaCl only. Also, a concentration dependent hygroscopic growth ($r_{70/80}$) was measured for particles containing Tergitol NP-40 and Brij L4 but not for particles containing Brij 35. The addition of Tergitol NP-40 and Brij L4 to aqueous NaCl at 1.5% surfactant mass fraction showed a statistically significantly enhanced water uptake (4% lower $r_{70/r80}$) compared to particles with a 0.5% surfactant mass fraction, as well as aqueous particles containing NaCl only. This shows that the type of surfactant as well as its mass fraction in the NaCl particle both play a role in the particle hygroscopic growth.

For the more complex, model SSA consisting of NaCl plus an organic fraction of surfactant and glucose, the particles were less hygroscopic (higher $r_{70/r80}$) than the corresponding NaCl-surfactant particles with the same surfactant mass fraction. This trend was observed for particles containing all three nonionic surfactants, but it is more pronounced for those particles containing Brij L4 or Tergitol NP-40. For these particles, the measured $r_{70/r80}$ is nearly equal to that of the aqueous NaCl only particles. This shows that a soluble organic, even at a small mass fraction, can counteract the effect of a surfactant on particle hygroscopic growth. This effect is likely due to a change in the

properties of the bulk solute of the particle. Glucose is not surface-active and thus should not influence the surfactant packing or concentration on the particle surface. However, it may change the surfactant micelle properties in the bulk of the particle.

Nonionic surfactants added to aqueous NaCl particles resulted in enhanced water uptake and larger particle sizes after growth under high humidity conditions, but the addition of glucose counteracted that effect. It is unlikely that atmospheric SSA contain only surfactants and inorganic salts, making the NaCl-surfactant-glucose particles studied here more atmospherically relevant than the NaCl-surfactant particles. In the atmosphere, if small fractions of soluble organics are present, in addition to small fractions of surfactants, the hygroscopic growth of supermicron particles will be most similar to that of pure inorganic salt particles. This is important for predicting the hygroscopic growth of supermicron particles and their contribution to the formation of fog, and thus decreased visibility, under high humidity conditions.

Further work is needed to evaluate the hygroscopic growth of more complex SSA and other types of atmospheric aerosol, including organic fractions with ranges of water solubilities mixed with surfactants with varying compositions. Future studies should incorporate a more complex breadth of organic compounds as well as varying organic mass fractions to measure their interactions with surfactants and the total effect on particle hygroscopic growth. Additionally, single particle surface tension measurements may help explain the interaction of surfactants and water-soluble organics in these particles. Evaluating the hygroscopic growth over a greater range of concentrations and chemical complexities will provide greater insight into the factors and mechanism that control the potential hygroscopic growth of supermicron atmospheric aerosol.

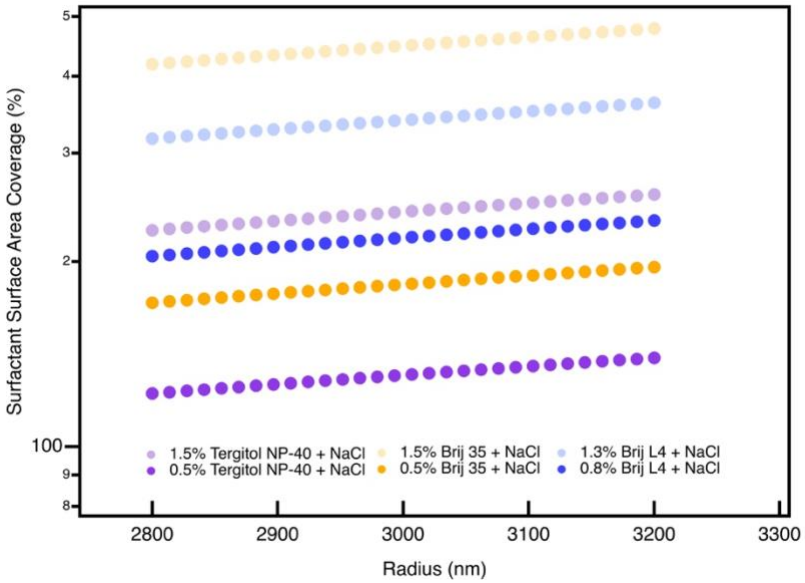

Figure S1. Comparison of the predicted percent nonionic surfactant surface area coverage across a range of experimentally relevant aqueous particle sizes at 80% relative humidity. Each color corresponds to a specific nonionic surfactant, while the different shades represent the different surfactant mass fractions. Calculations were only performed for the two-component particles that contain surfactant and NaCl. Glucose is assumed to have negligible surface-activity in the presence of surfactants and will not aggregate at the particle-air boundary

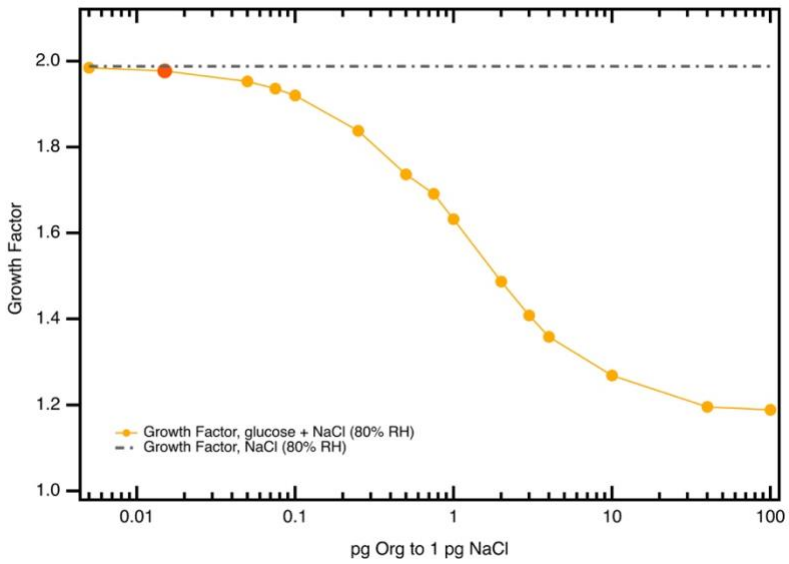

Figure S2. Growth factor curve for aqueous NaCl and glucose containing particles across a range of relevant mass fractions modeled by the Extended Inorganic-Organics Model (E-AIM). Single orange data point corresponds to the glucose:NaCl (0.015 : 1) mass fraction used in the aerosol optical trap (hygroscopic growth) experiments to calculate $r_{70/80}$. Grey dashed line represents the growth factor (0.91) for pure aqueous NaCl particles alone. At such dilute glucose concentrations, there is no deviation on the hygroscopic growth and the particle has a growth factor nearly equal to that of NaCl suggesting that the presence of glucose under these conditions has no influence on aerosol water uptake.

References

Abbatt, J. P. D., S. Benz, D. J. Cziczo, Z. Kanji, U. Lohmann, and O. Möhler. 2006. 'Solid Ammonium Sulfate Aerosols as Ice Nuclei: A Pathway for Cirrus Cloud Formation', *Science*, 313: 1770-73.

Attwood, David. 2009. *Modern Pharmaceutics Volume 1: Surfactants*.

Bain, Alison. 2024. 'Recent advances in experimental techniques for investigating aerosol surface tension', *Aerosol Science and Technology*, 58: 1213-36.

Bain, Alison, Kunal Ghosh, Nønne L. Prisle, and Bryan R. Bzdek. 2023. 'Surface-Area-to-Volume Ratio Determines Surface Tensions in Microscopic, Surfactant-Containing Droplets', *ACS Central Science*, 9: 2076-83.

Bain, Alison, Lara Lalemi, Nathan Croll Dawes, Rachael E. H. Miles, Alexander M. Prophet, Kevin R. Wilson, and Bryan R. Bzdek. 2024. 'Surfactant Partitioning Dynamics in Freshly Generated Aerosol Droplets', *Journal of the American Chemical Society*, 146: 16028-38.

Bertram, Timothy H., Richard E. Cochran, Vicki H. Grassian, and Elizabeth A. Stone. 2018. 'Sea spray aerosol chemical composition: elemental and molecular mimics for laboratory studies of heterogeneous and multiphase reactions', *Chemical Society Reviews*, 47: 2374-400.

Burdette, Tret C., Rachel L. Bramblett, Kathryn Zimmermann, and Amanda A. Frossard. 2023. 'Influence of Air Mass Source Regions on Signatures of Surface-Active Organic Molecules in Size Resolved Atmospheric Aerosol Particles', *ACS Earth and Space Chemistry*, 7: 1578-91.

Bzdek, Bryan R., Jonathan P. Reid, Jussi Malila, and Nønne L. Prisle. 2020. 'The surface tension of surfactant-containing, finite volume droplets', *Proceedings of the National Academy of Sciences*, 117: 8335-43.

Clegg, Simon L., John H. Seinfeld, and Peter Brimblecombe. 2001. 'Thermodynamic modelling of aqueous aerosols containing electrolytes and dissolved organic compounds', *Journal of Aerosol Science*, 32: 713-38.

Cui, Xiaohong, Shizhen Mao, Maili Liu, Hanzhen Yuan, and Youru Du. 2008. 'Mechanism of Surfactant Micelle Formation', *Langmuir*, 24: 10771-75.

David, Grégory, Evelyne A. Parmentier, Irene Taurino, and Ruth Signorell. 2020. 'Tracing the composition of single e-cigarette aerosol droplets in situ by laser-trapping and Raman scattering', *Scientific Reports*, 10: 7929.

de Leeuw, Gerrit, Edgar L Andreas, Magdalena D. Anguelova, C. W. Fairall, Ernie R. Lewis, Colin O'Dowd, Michael Schulz, and Stephen E. Schwartz. 2011. 'Production flux of sea spray aerosol', *Reviews of Geophysics*, 49.

Diamant, Haim, Gil Ariel, and David Andelman. 2001. 'Kinetics of surfactant adsorption: the free energy approach', *Colloids and Surfaces A: Physicochemical and Engineering Aspects*, 183-185: 259-76.

Eastoe, J., and J. S. Dalton. 2000. 'Dynamic surface tension and adsorption mechanisms of surfactants at the air–water interface', *Advances in Colloid and Interface Science*, 85: 103-44.

El Haber, Manuella, Corinne Ferronato, Anne Giroir-Fendler, Ludovic Fine, and Barbara Nozière. 2023. 'Salting out, non-ideality and synergism enhance surfactant efficiency in atmospheric aerosols', *Scientific Reports*, 13: 20672.

English, Jason M., Jennifer E. Kay, Andrew Gettelman, Xiaohong Liu, Yong Wang, Yuying Zhang, and Helene Chepfer. 2014. 'Contributions of Clouds, Surface Albedos, and Mixed-Phase Ice Nucleation Schemes to Arctic Radiation Biases in CAM5', *Journal of Climate*, 27: 5174-97.

Frossard, Amanda A., Violaine Gérard, Patrick Duplessis, Joanna D. Kinsey, Xi Lu, Yuting Zhu, John Bisgrove, John R. Maben, Michael S. Long, Rachel Y. W. Chang, Steven R. Beaupré, David J. Kieber, William C. Keene, Barbara Nozière, and Ronald C. Cohen. 2019. 'Properties of Seawater Surfactants Associated with Primary Marine Aerosol Particles Produced by Bursting Bubbles at a Model Air–Sea Interface', *Environmental Science & Technology*, 53: 9407-17.

Frossard, Amanda A., Wayne Li, Violaine Gérard, Barbara Nozière, and Ronald C. Cohen. 2018. 'Influence of surfactants on growth of individual aqueous coarse mode aerosol particles', *Aerosol Science and Technology*, 52: 459-69.

Gen, Masao, Akihide Hibara, Phuong Nguyet Phung, Yuzo Miyazaki, and Michihiro Mochida. 2023. 'In Situ Surface Tension Measurement of Deliquesced Aerosol Particles', *The Journal of Physical Chemistry A*, 127: 6100-08.

Gérard, Violaine, Barbara Nozière, Christine Baduel, Ludovic Fine, Amanda A. Frossard, and Ronald C. Cohen. 2016. 'Anionic, Cationic, and Nonionic Surfactants in Atmospheric Aerosols from the Baltic Coast at Askö, Sweden: Implications for Cloud Droplet Activation', *Environmental Science & Technology*, 50: 2974-82.

Haddrell, Allen E., Rachael E. H. Miles, Bryan R. Bzdek, Jonathan P. Reid, Rebecca J. Hopkins, and Jim S. Walker. 2017. 'Coalescence Sampling and Analysis of Aerosols using Aerosol Optical Tweezers', *Analytical Chemistry*, 89: 2345-52.

Haywood, J. M., and K. P. Shine. 1995. 'The effect of anthropogenic sulfate and soot aerosol on the clear sky planetary radiation budget', *Geophysical Research Letters*, 22: 603-06.

Haywood, James, and Olivier Boucher. 2000. 'Estimates of the direct and indirect radiative forcing due to tropospheric aerosols: A review', *Reviews of Geophysics*, 38: 513-43.

Holcomb, Cynthia D., and John A. Zollweg. 1992. 'Improved differential bubble pressure surface tensiometer', *Journal of Colloid and Interface Science*, 154: 51-65.

Hopkins, Rebecca J., Laura Mitchem, Andrew D. Ward, and Jonathan P. Reid. 2004. 'Control and characterisation of a single aerosol droplet in a single-beam gradient-force optical trap', *Physical Chemistry Chemical Physics*, 6: 4924-27.

Hua, Xi Yuan, and Milton J. Rosen. 1991. 'Dynamic surface tension of aqueous surfactant solutions: 3. Some effects of molecular structure and environment', *Journal of Colloid and Interface Science*, 141: 180-90.

Intergovernmental Panel on Climate, Change. 2014. *Climate Change 2013 – The Physical Science Basis: Working Group I Contribution to the Fifth Assessment Report of the Intergovernmental Panel on Climate Change* (Cambridge University Press: Cambridge).

Jacobs, Michael I., Madelyn N. Johnston, and Shahriar Mahmud. 2024. 'Exploring How the Surface-Area-to-Volume Ratio Influences the Partitioning of Surfactants to the Air–Water Interface in Levitated Microdroplets', *The Journal of Physical Chemistry A*, 128: 9986-97.

Jimenez, J. L., M. R. Canagaratna, N. M. Donahue, A. S. H. Prevot, Q. Zhang, J. H. Kroll, P. F. DeCarlo, J. D. Allan, H. Coe, N. L. Ng, A. C. Aiken, K. S. Docherty, I. M. Ulbrich, A. P. Grieshop, A. L. Robinson, J. Duplissy, J. D. Smith, K. R. Wilson, V. A. Lanz, C. Hueglin, Y. L. Sun, J. Tian, A. Laaksonen, T. Raatikainen, J. Rautiainen, P. Vaattovaara, M. Ehn, M. Kulmala, J. M. Tomlinson, D. R. Collins, M. J. Cubison, E., J. Dunlea, J. A. Huffman, T.

B. Onasch, M. R. Alfarra, P. I. Williams, K. Bower, Y. Kondo, J. Schneider, F. Drewnick, S. Borrmann, S. Weimer, K. Demerjian, D. Salcedo, L. Cottrell, R. Griffin, A. Takami, T. Miyoshi, S. Hatakeyama, A. Shimono, J. Y Sun, Y. M. Zhang, K. Dzepina, J. R. Kimmel, D. Sueper, J. T. Jayne, S. C. Herndon, A. M. Trimborn, L. R. Williams, E. C. Wood, A. M. Middlebrook, C. E. Kolb, U. Baltensperger, and D. R. Worsnop. 2009. 'Evolution of Organic Aerosols in the Atmosphere', *Science*, 326: 1525-29.

Keene, William C., Hal Maring, John R. Maben, David J. Kieber, Alexander A. P. Pszenny, Elizabeth E. Dahl, Miguel A. Izaguirre, Andrew J. Davis, Michael S. Long, Xianliang Zhou, Linda Smoydzin, and Rolf Sander. 2007. 'Chemical and physical characteristics of nascent aerosols produced by bursting bubbles at a model air-sea interface', *Journal of Geophysical Research: Atmospheres*, 112.

Kleefeld, Christoph, Colin D. O'Dowd, Sarah O'Reilly, S. Gerard Jennings, Pasi Aalto, Edo Becker, Gerard Kunz, and Gerrit de Leeuw. 2002. 'Relative contribution of submicron and supermicron particles to aerosol light scattering in the marine boundary layer', *Journal of Geophysical Research: Atmospheres*, 107: PAR 8-1-PAR 8-13.

Knopf, Daniel A., Peter A. Alpert, and Bingbing Wang. 2018. 'The Role of Organic Aerosol in Atmospheric Ice Nucleation: A Review', *ACS Earth and Space Chemistry*, 2: 168-202.

Knox, K. J., J. P. Reid, K. L. Hanford, A. J. Hudson, and L. Mitchem. 2007. 'Direct measurements of the axial displacement and evolving size of optically trapped aerosol droplets', *Journal of Optics A: Pure and Applied Optics*, 9: S180-S88.

Köhler, Hilding. 1936. 'The nucleus in and the growth of hygroscopic droplets', *Transactions of the Faraday Society*, 32: 1152-61.

Koneva, Alina S., Eric Ritter, Yuri A. Anufrikov, Alexey A. Lezov, Anastasiya O. Klestova, Natalia A. Smirnova, Evgenia A. Safonova, and Irina Smirnova. 2018. 'Mixed aqueous solutions of nonionic surfactants Brij 35/Triton X-100: Micellar properties, solutes' partitioning from micellar liquid chromatography and modelling with COSMOmic', *Colloids and Surfaces A: Physicochemical and Engineering Aspects*, 538: 45-55.

Lewis, Ernie R., and Stephen E. Schwartz. 2004. 'Fundamentals.' in, *Sea Salt Aerosol Production: Mechanisms, Methods, Measurements and Models*.

Lohmann, U., and J. Feichter. 2005. 'Global indirect aerosol effects: a review', *Atmos. Chem. Phys.*, 5: 715-37.

Maibaum, Lutz, Aaron R. Dinner, and David Chandler. 2004. 'Micelle Formation and the Hydrophobic Effect', *The Journal of Physical Chemistry B*, 108: 6778-81.

Malila, J., and N. L. Prisle. 2018. 'A Monolayer Partitioning Scheme for Droplets of Surfactant Solutions', *Journal of Advances in Modeling Earth Systems*, 10: 3233-51.

Mazoyer, M., F. Burnet, C. Denjean, G. C. Roberts, M. Haeffelin, J. C. Dupont, and T. Elias. 2019. 'Experimental study of the aerosol impact on fog microphysics', *Atmos. Chem. Phys.*, 19: 4323-44.

Mitchem, Laura, Jariya Buajarern, Rebecca J. Hopkins, Andrew D. Ward, Richard J. J. Gilham, Roy L. Johnston, and Jonathan P. Reid. 2006. 'Spectroscopy of Growing and Evaporating Water Droplets: Exploring the Variation in Equilibrium Droplet Size with Relative Humidity', *The Journal of Physical Chemistry A*, 110: 8116-25.

Mitchem, Laura, and Jonathan P. Reid. 2008. 'Optical manipulation and characterisation of aerosol particles using a single-beam gradient force optical trap', *Chemical Society Reviews*, 37: 756-69.

Miyazaki, Yuzo, Youhei Yamashita, Kaori Kawana, Eri Tachibana, Sara Kagami, Michihiro Mochida, Koji Suzuki, and Jun Nishioka. 2018. 'Chemical transfer of dissolved organic matter from surface seawater to sea spray water-soluble organic aerosol in the marine atmosphere', *Scientific Reports*, 8: 14861.

O'Dowd, Colin D, and Gerrit de Leeuw. 2007. 'Marine aerosol production: a review of the current knowledge', *Philosophical Transactions of the Royal Society A: Mathematical, Physical and Engineering Sciences*, 365: 1753-74.

O'Dowd, Colin D., Maria Cristina Facchini, Fabrizia Cavalli, Darius Ceburnis, Mihaela Mircea, Stefano Decesari, Sandro Fuzzi, Young Jun Yoon, and Jean-Philippe Putaud. 2004. 'Biogenically driven organic contribution to marine aerosol', *Nature*, 431: 676-80.

Paramonov, M., P. P. Aalto, A. Asmi, N. Prisle, V. M. Kerminen, M. Kulmala, and T. Petäjä. 2013. 'The analysis of size-segregated cloud condensation nuclei counter (CCNC) data and its implications for cloud droplet activation', *Atmos. Chem. Phys.*, 13: 10285-301.

Quinn, Patricia K., Douglas B. Collins, Vicki H. Grassian, Kimberly A. Prather, and Timothy S. Bates. 2015. 'Chemistry and Related Properties of Freshly Emitted Sea Spray Aerosol', *Chemical Reviews*, 115: 4383-99.

Rosen, Milton J. 1972. 'The relationship of structure to properties in surfactants', *Journal of the American Oil Chemists' Society*, 49: 293-97.

———. 2004. 'Micelle Formation by Surfactants.' in, *Surfactants and Interfacial Phenomena*.

Summers, M. D., J. P. Reid, and D. McGloin. 2006. 'Optical guiding of aerosol droplets', *Optics Express*, 14: 6373-80.

Swanson, Benjamin E., and Amanda A. Frossard. 2022. 'Influence of selected cationic, anionic, and nonionic surfactants on hygroscopic growth of individual aqueous coarse mode aerosol particles', *Aerosol Science and Technology*, 57: 63-76.

Tang, I. N., A. C. Tridico, and K. H. Fung. 1997. 'Thermodynamic and optical properties of sea salt aerosols', *Journal of Geophysical Research: Atmospheres*, 102: 23269-75.

Vaccaro, Ralph F., Sonja E. Hicks, Holger W. Jannasch, and Francis G. Carey. 1968. 'THE OCCURRENCE AND ROLE OF GLUCOSE IN SEAWATER', *Limnology and Oceanography*, 13: 356-60.

Warmbier, Ewelina, Ali Altaee, Jacek Różański, Tayma Kazwini, Sylwia Różańska, Ibrar Ibrar, Patrycja Wagner, Maryam Al-Ejji, and Alaa H. Hawari. 2024. 'Stability of Viscoelastic Solutions: BrijL4 and Sodium Cholate Mixtures with Metal Ions Across a Broad pH and Temperature Range', *Langmuir*, 40: 1707-16.

Werner, Emily K., Makaila Hammond, and Alison Bain. 2025. 'Surface tension predictions during hygroscopic growth and cloud droplet activation using a simple kinetic surfactant partitioning model', *Aerosol Science and Technology*, 59: 781-93.

Wills, Jon B., Kerry J. Knox, and Jonathan P. Reid. 2009. 'Optical control and characterisation of aerosol', *Chemical Physics Letters*, 481: 153-65.

Xi Yuan, Hua, and Milton J. Rosen. 1988. 'Dynamic surface tension of aqueous surfactant solutions: I. Basic paremeters', *Journal of Colloid and Interface Science*, 124: 652-59.

Yu, H., Y. J. Kaufman, M. Chin, G. Feingold, L. A. Remer, T. L. Anderson, Y. Balkanski, N. Bellouin, O. Boucher, S. Christopher, P. DeCola, R. Kahn, D. Koch, N. Loeb, M. S. Reddy, M. Schulz, T. Takemura, and M. Zhou. 2006. 'A review of measurement-based assessments of the aerosol direct radiative effect and forcing', *Atmos. Chem. Phys.*, 6: 613-66.

Zhang, Xiaolu, Paola Massoli, Patricia K. Quinn, Timothy S. Bates, and Christopher D. Cappa. 2014. 'Hygroscopic growth of submicron and supermicron aerosols in the marine boundary layer', *Journal of Geophysical Research: Atmospheres*, 119: 8384-99.

Zuend, A., C. Marcolli, B. P. Luo, and T. Peter. 2008. 'A thermodynamic model of mixed organic-inorganic aerosols to predict activity coefficients', *Atmos. Chem. Phys.*, 8: 4559-93.